# From Confidence to Collapse in LLM Factual Robustness

# Alina Fastowski Bardh Prenkaj Gjergji Kasneci

Technical University of Munich {name.surname}@tum.de

### **Abstract**

Ensuring the robustness of factual knowledge in LLMs is critical for reliable applications in tasks such as question answering and reasoning. However, existing evaluation methods predominantly focus on performance-based metrics, often investigating from the perspective of prompt perturbations, which captures only the externally triggered side of knowledge robustness. To bridge this gap, we introduce a principled approach to measure factual robustness from the perspective of the generation process by analyzing token distribution entropy in combination with temperature scaling sensitivity. These two factors build the Factual Robustness Score (FRS), a novel metric which quantifies the stability of a fact against perturbations in decoding conditions, given its initial uncertainty. To validate our approach, we conduct extensive experiments on 5 LLMs across 3 closed-book QA datasets (SQuAD, TriviaQA, and HotpotQA). We show that factual robustness varies significantly - smaller models report an FRS of 0.76, larger ones 0.93 – with accuracy degrading by  $\sim 60\%$  under increased uncertainty. These insights demonstrate how entropy and temperature scaling impact factual accuracy, and lay a foundation for developing more robust knowledge retention and retrieval in future models. We release our code at https://github.com/afastowski/frs.

### 1 Introduction

Large Language Models (LLMs) have revolutionized natural language understanding and generation, demonstrating remarkable capabilities across tasks such as question answering, knowledge-intensive text generation, and reasoning (Petroni et al., 2019; Roberts et al., 2020; Hu et al., 2023). However, despite their strong performance, factual stability remains an open challenge. While a model may provide a correct answer under one set of decoding conditions, it may fail to do so when

faced with minor perturbations, such as variations in sampling temperature. This raises a fundamental question: how robustly is factual knowledge embedded in LLMs?

Traditional evaluations of factual knowledge in LLMs rely on accuracy-based metrics, which measure correctness under fixed conditions (Joshi et al., 2017; Kwiatkowski et al., 2019; Hendrycks et al., 2021). However, these methods do not account for uncertainty in fact retrieval – whether a model is inherently confident in its answer or if its correctness is fragile under perturbations. Additionally, prior techniques often focus on single-temperature evaluations, failing to systematically analyze how factual outputs degrade as uncertainty is introduced (Maynez et al., 2020; Gabriel et al., 2021). To bridge this gap, we introduce a novel perspective: factual robustness, which examines not just whether an answer is correct but how resistant it is to internal uncertainty and temperature-induced variability.

To quantify this, we propose the Factual Robustness Score (FRS), a new metric designed to measure the stability of factual knowledge within an LLM. Unlike previous work that assesses model performance at isolated temperature values, FRS integrates both entropy and temperature, providing a comprehensive robustness assessment. Entropy quantifies the model's intrinsic confidence in an answer, while the so-called "breaking" temperature is the first temperature greater than zero, at which the generation produces an incorrect answer. In other words, it captures how much uncertainty the generation process can withstand, before shifting from the correctly produced answer to an incorrect one. By combining these two dimensions, FRS moves beyond simple accuracy and provides a deeper insight into how reliably knowledge is stored and retrieved within LLMs.

Through extensive experiments across multiple LLM architectures and datasets, we show that higher-entropy facts degrade more under temperature perturbations, while lower-entropy facts remain more stable. Model size alone does not dictate robustness, as architectural and training differences also play a role. Additionally, factual stability varies by knowledge type, with numerical facts proving more resilient than others.

Our contributions are multifold:

- We introduce the Factual Robustness Score (FRS), the first metric to systematically assess the stability of factual knowledge in LLMs by integrating entropy and breaking temperature.
- We analyze the impact of temperature on factual accuracy, showing that increasing temperature systematically degrades correctness, but that this effect varies across models and knowledge types.
- We provide empirical evidence that factual robustness is not solely determined by model size, highlighting the role of architecture and training methods in knowledge stability.
- 4. We identify variations in robustness across different types of factual knowledge, showing that certain categories, such as numerical facts, are more resilient than others.
- We demonstrate that factual robustness cannot be inferred from accuracy alone, reinforcing the need for stability-focused evaluation methods beyond traditional correctness assessments.

### 2 Preliminaries

**Entropy** is a measure of disorder and randomness in a system. In text generation, it measures the spread of the probability distribution over possible tokens, with higher entropy indicating more randomness, and lower entropy reflecting more confident, deterministic predictions (see Equation (1)). Following the intuition of entropy, we consider it as the first factor in our robustness assessments.

$$H = -\sum_{i} P(x_i) \log P(x_i). \tag{1}$$

**Temperature** is a parameter that controls the sharpness of the probability distribution during text generation. It operates by scaling the logits before applying the softmax, as defined in Equation (2):

$$P(x_i;t) = \frac{\exp\left(\frac{\log P(x_i)}{\max(t,\varepsilon \cdot \mathbb{1}_{t=0})}\right)}{\sum_{j} \exp\left(\frac{\log P(x_j)}{\max(t,\varepsilon \cdot \mathbb{1}_{t=0})}\right)},$$
 (2)

where  $t \geq 0$  is the temperature value,  $\varepsilon > 0$  is a small number approaching 0, in our experiments set to  $10^{-4}$ , to avoid zero divisions, and  $\mathbb{1}_{t=0}$  is the indicator function with the condition t=0. A lower t makes the probability distribution more peaked, reinforcing the dominance of high-probability tokens and making the model more deterministic. Conversely, a higher temperature flattens the distribution, increasing the likelihood of selecting lower-probability tokens and promoting more diverse generations. The effect of temperature serves as the second factor in our robustness analysis.

**LLMs' True Factual Knowledge.** To assess factual robustness in LLMs, we first identify facts the model answers correctly at t=0, where the probability distribution is sharply peaked, ensuring the most likely tokens dominate (see Figure 2). If the model has high confidence in the correct answer, it will always produce it at t=0. However, as we increase the temperature towards t=1, the probability distribution flattens, allowing lower-probability tokens to be chosen. At t=1, temperature scaling no longer affects the probability computation (see Equation (2)), meaning we observe the model's intrinsic token distribution—its true knowledge representation, without artificially enforced certainty.

Our key idea is as follows: if an initially correct answer starts shifting to an incorrect one as we increase the temperature, the fact is not robustly stored in the model. In other words, if the model can only produce the correct answer when artificially forced into a low-uncertainty setting (t = 0), then the fact is not stably embedded in its knowledge base. A truly robust fact should remain correct across a range of temperatures, reflecting consistent and confident knowledge retention. Furthermore, the initial entropy of a generated answer gives another factor about its robustness: if an answer is produced at high uncertainty, it is less robust from the beginning. This leads us to introduce a novel measure, which incorporates both of these factors the Factual Robustness Score (FRS) – which is further detailed in Section 5.

#### 3 Related Work

### 3.1 Factual Knowledge in Language Models

LLMs encode vast amounts of factual knowledge, often retrieved from internal representations rather than structured databases. While models can recall these facts, their responses remain inconsis-

tent, suffering from hallucinations and retrieval errors (Petroni et al. (2019), Roberts et al. (2020)). A prominent research direction focuses on understanding and modifying how knowledge is encoded within LLMs: while Geva et al. (2020) and Dai et al. (2021) identified specific structures within Transformers, such as key-value memory stores and knowledge neurons, De Cao et al. (2021) and Meng et al. (2022) explored techniques to directly manipulate the information stored within model weights. However, beyond the challenge of modifying knowledge, ensuring its stability and reliability remains an open problem. While Zong et al. (2024) introduced ComparisonQA to evaluate factual robustness under controlled knowledge frequency and uncertainty, a broader body of work has framed robustness through the lens of adversarial attacks. Studies such as Xu et al. (2024), Bondarenko and Viehweger (2024), and Howe et al. (2024) have examined the vulnerability of LLMs to prompt-side perturbations, revealing inconsistencies in factual recall. Approaching the question through the prompt lens, Mahaut et al. (2024) consider factual robustness in terms of semantically equivalent question phrasing. Contrary to the approaches above, our work shifts the focus from external prompt modifications to the model-side of the generation process, investigating the internal mechanisms that contribute to factual robustness.

### 3.2 Temperature and Language Models

While seemingly distant from modern LLMs, Ackley et al. (1985) established temperature as a key factor in shaping probability distributions, a principle still central to language model decoding today. Recent studies have debated whether temperature significantly impacts problem-solving ability. Renze and Guven (2024) found that varying temperature from 0.0 to 1.6 had no significant effect on accuracy, challenging the assumption that lower temperatures enhance reasoning. Beyond accuracy, temperature is often associated with creativity: Peeperkorn et al. (2024) showed that while higher temperatures increase variation, this does not necessarily translate into meaningful novelty, raising questions about its role.

Recognizing the limitations of fixed-temperature sampling, researchers have developed adaptive temperature control strategies to balance quality and diversity. Chang et al. (2023) introduced KL-Divergence Guided Temperature Sampling, which

adjusts temperature dynamically based on token relevance, while Zhang et al. (2024) proposed Entropy-based Dynamic Temperature (EDT) Sampling to optimize fluency and diversity.

A novel perspective on temperature scaling comes from Nakaishi et al. (2024), who found that LLMs undergo critical phase transitions at certain temperature thresholds, exhibiting abrupt behavioral shifts akin to phase changes in physical systems. This suggests that temperature adjustments do more than refine probability distributions – they can fundamentally reshape generative dynamics, making temperature a key factor in understanding LLM computational behavior.

Our Contribution. Unlike existing performance-based methods that assess correctness at fixed temperatures, or studies in attack-based scenarios, we evaluate how robustly a fact is stored within a model by incorporating both entropy and "breaking" temperature – the temperature at which a model switches to producing an incorrect answer. This allows for a more comprehensive assessment of factual stability, moving beyond surface-level correctness to quantify how knowledge withstands perturbations in sampling conditions. Our work provides new insights into the resilience of LLMs and highlights the need for robustness-focused evaluation metrics in future research.

### 4 Experiments and Results

### 4.1 Experimental Setup

### 4.1.1 Closed-Book Question Answering Setup

Our study operates within a closed-book question answering (QA) setting, where models generate answers based solely on the input question, without access to external documents or retrieval mechanisms. This ensures that any correctly answered question reflects knowledge stored within the model's parameters.

**Datasets.** We use three widely studied QA datasets, each adjusted for the closed-book setting: (1) SQuAD (Rajpurkar et al., 2016), a reading comprehension dataset primarily composed of Wikipediabased questions; (2) TriviaQA (Joshi et al., 2017), a collection of knowledge-intensive questions originally designed for open-domain QA; and (3) HotpotQA (Yang et al., 2018), a multi-hop QA dataset that requires reasoning over multiple facts.

**Model Selection.** To ensure diversity in model architectures, scales, and training sources, we eval-

uate five different LLMs: i.e., GPT-4o-mini (OpenAI, 2023), LLaMA-3.2-3B and LLaMA-3.1-8B (Touvron et al., 2023), Qwen-2.5-3B and Qwen-2.5-14B (Yang et al., 2024). The GPT models are accessed via the OpenAI API, while the LLaMA and Qwen models are loaded from Hugging Face, using their instruct fine-tuned versions.

Controlling Response Length and Format. To manage verbosity and enforce concise answers, we provide each model with two-shot exemplars – examples of questions paired with expected, brief responses – before prompting with the actual question. Additionally, we set max\_new\_tokens=5, limiting response length to a maximum of five tokens. This setup ensures that models produce concise, directly comparable outputs across datasets and temperature conditions, enabling a rigorous analysis of factual recall and response certainty.

# **4.1.2** Selection of Correctly Answered Ouestions for Analysis

To establish a controlled and reliable basis for our experiments, we begin by identifying 1000 correctly answered questions per dataset and model. This selection process ensures that our analysis focuses on instances where the model demonstrably possesses the required knowledge.

Baseline Selection Criteria. To identify these correctly answered questions, we set the generation temperature t to zero, enforcing deterministic output selection. This choice minimizes stochastic variability, ensuring that the most probable token sequence is always selected. Since we study model robustness, we are showing the effects of increasingly hard generation conditions. Hence, by first setting t = 0, we establish a baseline representing the model's most "ideal" conditions for factual retrieval. Additionally, to simulate a well-calibrated model, we filter out instances where the model confidently produces incorrect answers. This ensures that our study focuses solely on high-confidence correct responses, allowing us to analyze the impact of increasing temperature without confounding effects from miscalibrated predictions.

Inference and Selection Process. At inference time, the model generates a single response per question. We evaluate the output using an exact match criterion – if the generated answer is identical to the ground truth, the sample is retained as a correctly answered question. This guarantees that the model has the knowledge necessary to answer these questions correctly under optimal conditions.

By enforcing these selection criteria, we create a robust experimental foundation that allows us to systematically study the effects of increasing temperature on response accuracy and certainty.

### 4.2 Temperature Scaling

Temperature t is a key parameter in the generation process, controlling the level of randomness and semantic variability in model outputs. It theoretically ranges from 0 to  $\infty$ , although it is typically constrained between 0 and 2 (Renze and Guven, 2024). Recall that lower temperatures lead to more deterministic outputs, while higher values introduce greater diversity by flattening the probability distribution. To systematically analyze the impact of temperature on response accuracy and certainty, we apply temperature scaling to the previously identified correctly answered questions for each model and dataset. The procedure is as follows:

- (1) For each question, we progressively increase t and observe performance variations.
- (2) Since generation is a probabilistic sampling process, we run each question 10 times per temperature setting to account for variability in model outputs.
- (3) A response is deemed correct if it contains the ground truth answer, allowing for minor verbosity while maintaining correctness beyond exact match. Accuracy is then calculated as the proportion of correct responses across 10 trials per question.

We evaluate  $t \in \{0.2, \ldots, 2.0\}$ , with steps of +0.2. This range ensures a balanced exploration of temperature effects, spanning from near-deterministic outputs to moderately diverse sampling regimes. The following results illustrate how temperature scaling influences factual robustness across different models and datasets.

Effects of Temperature on Factual Accuracy and Certainty Levels. As shown in Figure 1, accuracy consistently decreases with increasing temperature across all models and datasets. This decline is a direct consequence of higher temperature values amplifying probabilistic sampling, allowing less probable tokens to be selected more frequently. Notably, smaller models such as LLaMA-3b and LLaMA-8b experience the steepest declines, losing over 60% of their accuracy in some cases. In contrast, larger models like GPT-4o-mini and Qwen-14b demonstrate greater resilience, maintaining relatively higher accuracy at elevated temperatures. This trend suggests that model size and training

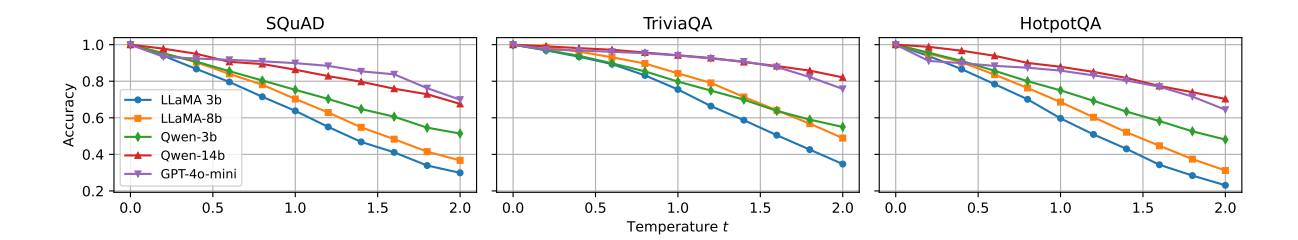


Figure 1: Accuracy steadily degrades with increasing temperature levels. We show that temperature is a direct factor in the difficulty of keeping the correct answer. Across all LLMs and datasets, accuracy decreases with increasing temperature, making temperature a direct factor in correct responses.

scale influence robustness to temperature-induced uncertainty, with larger models better preserving factual consistency despite increased stochasticity in token selection.

Furthermore, we analyze the certainty levels, in terms of token probability, of generated responses at varying temperature settings (Figure 2). Here, we compute the average probability of generated responses and categorize them into certainty bins.<sup>1</sup> This visualization clearly demonstrates how temperature scaling flattens the probability distribution, increasing competition among tokens and making the correct answer less consistently selected. Interestingly, even as temperature increases, some responses remain correct, indicating that certain facts are inherently more robust to temperature-induced variability. This observation suggests a potential for defining a temperature-based robustness met**ric**, where the level of t at which a correct answer "breaks" could serve as a measure of factual stability within the model.

### 4.3 Entropy of true distribution

Besides temperature, we analyze the entropy levels of generated answers to understand how entropy interacts with temperature-induced distribution shifts without compromising factual accuracy. To standardize our entropy measurements, we use  $\log_{10}$  instead of  $\log_2$ , ensuring that the maximum entropy value is fixed at 1. The theoretical upper bound of entropy for a given probability distribution is determined by  $\log(n)$ , where n represents the number of possible outcomes – in our case, the number of candidate tokens at a given position. Since we restrict the top token choices to  $10^2$ , the maximum

entropy value in our setup is  $\log_{10}(10) = 1$ .

Entropy vs. Breaking Temperature. We begin by analyzing the relationship between the baseline entropy of correct answers – i.e., the entropy over correctly generated tokens at t=0 – and the temperature at which these answers become incorrect due to token selection shifts. For each sample, we determine the first temperature level where the model's accuracy drops below a predefined threshold of 0.5, hence we say that the model "breaks". Once the breaking temperature  $t_b$  is identified for each sample, we compute the entropy of the originally correct answer's token distribution at t=0. Entropy is calculated at each token position and then averaged across all tokens in the answer, yielding a single entropy score per response.

### 4.4 Combining Entropy and Temperature

After establishing the relevance of both entropy and temperature scaling to the concept of factual robustness, we investigate the correlation between the two factors in Figure 3. The plots depict the initial entropy levels in relation to the breaking temperature. While there is a downward trend to be observed, the two variables do not exclusively predict each other. We show this by computing the Pearson Correlation between the two variables of initial entropy and breaking temperature, and find only a slight negative correlation for most models (-0.48 on average), while GPT-40-mini shows almost no correlation (-0.24 on average).

Since we show that these two concepts **do not express the same dimension of factual robustness** yet are both elementary to the robustness concept, we proceed to combine them into one solid Factual Robustness Score.

<sup>&</sup>lt;sup>1</sup>For example, the bin 0.7-0.8 includes all responses – correct or incorrect – whose average probability falls within the range [0.7, 0.8).

<sup>&</sup>lt;sup>2</sup>The restriction is necessary due to API limitations for GPT-40-mini. In order to be consistent, we apply the same limit to all models.

<sup>&</sup>lt;sup>3</sup>We define a significant degradation as an accuracy drop below 50%.

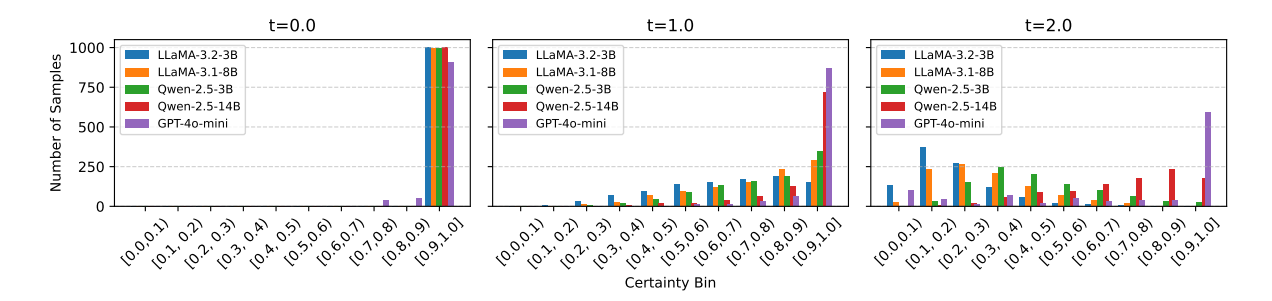


Figure 2: **Impact of temperature t on token probability distribution in TriviaQA**. As t increases, the probability distribution flattens, reducing certainty in token selection and increasing the likelihood of generating lower-probability responses. This highlights how temperature directly influences response confidence and factual stability.

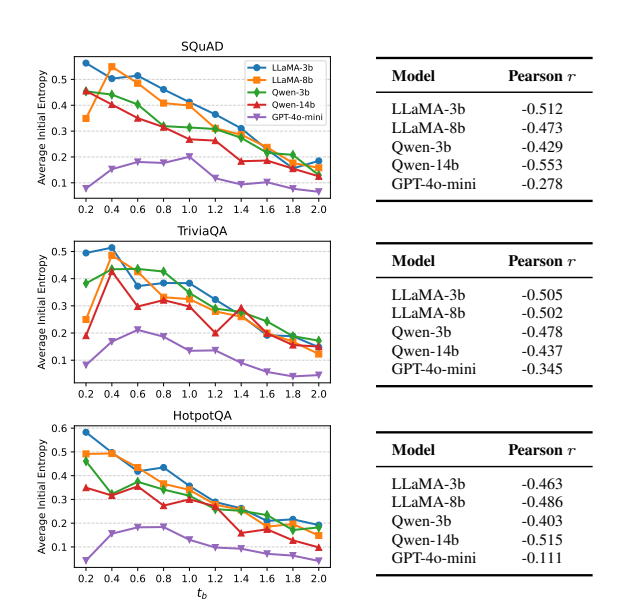


Figure 3: Average entropy levels of originally correct answers vs. the breaking temperature levels. While we observe a downward trend, we show that there is only a weak correlation between the initial entropy of an answer and its breaking temperature.

# 5 How Factually Robust are LLMs?

In contrast to the findings of Renze and Guven (2024), who argue that temperature has no significant impact, our results in Sections 4.2 and 4.3 demonstrate that increasing temperature in a QA context reduces both accuracy and certainty, regardless of model size. This sensitivity to temperature highlights the need for LLMs to maintain factual reliability under varying generation conditions.

Our goal is to provide a quantitative measure of factual robustness in LLMs. To this end, we introduce the Factual Robustness Score (FRS), which captures the stability of factual knowledge and its resilience to distributional shifts. From our perspective, a fact's robustness depends on two key

factors: (1) the model's initial uncertainty (entropy) when generating the fact at t=0, and (2) its resistance to perturbations as temperature increases. By integrating both aspects, we propose FRS as a single, comprehensive score that quantifies how well an LLM retains factual knowledge under varying temperature sampling conditions.

### 5.1 Factual Robustness Score (FRS)

**Initial Confidence.** We quantify the model's initial certainty by  $(1-H)^d$  where  $H \in [0,1]$  is the entropy – scaled so that H=1 means high uncertainty and H=0 means high confidence – and  $d \geq 1$  tunes how strictly we penalize uncertainty – i.e., larger d penalizes even moderate H more severely.

**Temperature Resilience.** Let  $t_b \geq 0$  be the smallest temperature at which the model's accuracy drops below a chosen threshold (e.g., 50%). We refer to it as the *breaking temperature*. If  $t_b$  is large, the model remains correct under stronger sampling perturbations and should receive a higher score. To capture this, we include the factor  $(t_b+1)$ .

**Entropy-Based Penalty.** Even if the model can withstand high temperatures, large H indicates the model is essentially "guessing." Hence we subtract a penalty proportional to H. For scale consistency, we divide by  $(t_b+1)$  to reduce the penalty when  $t_b$  is large: i.e.,  $\frac{H}{t_b+1}$ .

Constructing the Final Formula. We combine the "reward" and the "penalty" into a single function  $f: \mathbb{R}^1_0 \times \mathbb{R}_+ \times \mathbb{R}_+ \to \mathbb{R}$ :

$$f(H,d,t_b) = (1-H)^d \cdot (t_b+1) - \frac{H}{t_b+1}.$$
 (3)

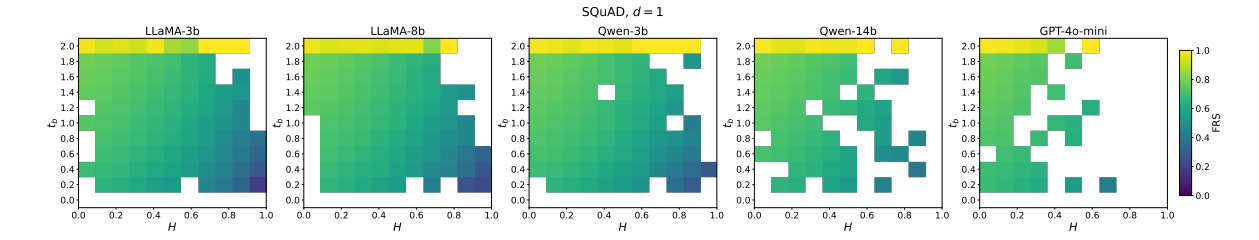


Figure 4: FRS (d=1) over all models, on SQuAD. Although FRS equal to 1 is theoretically achievable when  $t_b \to \infty$ , in practice, we set it to 1 for all samples where models did not break with  $t_b \le 2$ . Hence, the yellow data points.

Table 1: Average FRS with  $d \in \{1, 2, 5, 10, 50\}$  across all datasets. Generally larger **models are more robust** than smaller ones. \* indicates the most robust model overall.

d	LLaMA-3b	LLaMA-8b	Qwen-3b	Qwen-14b *	GPT-4o-mini
1	0.761	0.812	0.855	0.935	0.923
2	0.727	0.787	0.836	0.928	0.919
5	0.669	0.741	0.799	0.913	0.910
10	0.629	0.706	0.771	0.898	0.900
50	0.587	0.663	0.740	0.878	0.875

Since  $f(H, d, t_b) \in [-1, \infty)$  – see Appendix B.1 – we slightly modify Equation (3) to have a more interpretable score of factual robustness by balancing initial knowledge confidence (entropy) with resilience to temperature perturbations as follows:

$$f(H,d,t_b)_0^1 = \frac{f(H,d,t_b) + 1}{f(H,d,t_b) + 2}.$$
 (4)

We refer the reader to Appendix B.2 for a step-bystep derivation of Equation (4).

**Intuition of FRS.** We further visualize the intuition behind the function in Equation (3) and how the entropy is a weighting factor over the breaking temperature (see Appendix C). Recall that a model retains a fact if it obtains at least 50% accuracy in answering over 10 trials; otherwise, it breaks. When  $H \approx 0$  (high confidence) and  $t_b$ is large (breaks late), f becomes large. When  $H \approx 1$  (no confidence),  $(1-H)^d \approx 0$  and  $H/(t_b+1)\approx 1/(t_b+1)$ , so f is near zero or negative. Increasing d tightens the penalty on any uncertainty H > 0, reflecting stricter requirements for robust factual knowledge. This derivation shows how  $f(H, d, t_h)$  cleanly fuses how confident a model is in a fact with how long it withstands temperature perturbations, thus producing a single measure of factual robustness.

### 5.2 Model Family vs. Size in Robustness

Table 1 compares FRS across different model sizes and families using various values of  $d \in$  $\{1, 2, 5, 10, 50\}$ , controlling the influence of the entropy. As expected, larger models generally tend to be more robust than their smaller counterparts. However, a particularly interesting finding is that model size alone is not the sole predictor of robustness across different model families. While larger models within the same family (e.g., LLaMA-3b vs. LLaMA-8b) tend to retain facts more reliably, comparing across families (e.g., LLaMA vs. Qwen) introduces additional factors beyond just model size. Even though LLaMA-8b exhibits a more stable entropy trend in relation to  $t_b$  (see Figure 3), the smaller Qwen-3b model actually achieves a higher average FRS. Interesting in this context is also GPT-40-mini, which, being an 8 billion parameters model, has similarly high robustness as the leader, Qwen-14b. Hence, we argue that different models store and retrieve factual knowledge in distinct ways. While parameter size plays a central role in a model's factual robustness, factors like model architecture and training data may also be defining factors.

We also show how the FRS gets hampered with an increasing d based on the initial entropy. Notice how the LLaMA models suffer the highest drop in FRS (-0.174 for 3b, and -0.149 for 8b), meaning that they were uncertain, on average, about the initial factual knowledge, confirmed in Figure 1 where LLaMA has the highest accuracy drop across the board. To explore this further, Figure 4 illustrates FRS with d=1 across all models on the SQuAD dataset. Notably, Qwen-14b achieves higher FRS scores even when its initial entropy is lower than that of GPT-4o-mini, whereas the latter's scores are more concentrated toward the lower entropy range. Additionally, GPT-4o-mini exhibits a more skewed probability density distribution, with FRS  $\rightarrow 1$ ,

suggesting that while it may be highly confident in certain cases, its robustness is not consistently superior across all factual scenarios (see Appendix G). These findings highlight the need for a deeper examination into how architectures, training methodologies, and knowledge retention influence factual robustness.

#### 5.3 Most and Least Robust Facts

We further analyze the specific question types that are the most and least robust within the models. For this, we choose to fine-tune a lightweight classifier, DistilBERT (Sanh et al., 2019), on the TREC question type dataset (Li and Roth, 2002) to classify the categories Numerical, Location, Entity and Human, for which we reach 96,6% accuracy on the test set.<sup>4</sup> We then collect the top 1000 highest and lowest FRS score samples across all datasets, for each model. For both the top and bottom samples, we compute the proportion of each question type relative to the total number of samples of that type. Figure 5 shows the ratio of the most robust question types in percentage for each model. For example, for LLaMA-3B, 64.8% of numerical type questions are among the most robust (while 100% - 64.8% = 35.2% are part of the least robust). Answers associated with numerical and location related questions tend to be the most robust across models, reaching up to 72.9% and 64.9%, respectively. The least robust answers belong to the Human entity type, which means questions asking about the name of a person or a group. We show that all models recall names in a less robust way, meaning that those are most prone to be produced with high entropy and/or are shifting to a wrong answer at low temperature levels. We hypothesize that this is due to the nature of expected answers: for example, questions of the numerical type most often call for a single digit as answer, e.g., a year. Here, the LLM has less individual tokens to produce, and hence less chance of introducing an error, than for example with the name of a person, which is more lengthy. It is furthermore interesting to note the difference between model sizes: while the bigger models perform highest on numerical type questions, they underperform smaller models like LLaMA-3B on human type questions.

We want to emphasize that this study is not about certain LLMs performing better or worse on answering specific question types, but **the robustness**  **of their answers**, which, according to our study, does not always directly correspond to model size and capabilities.

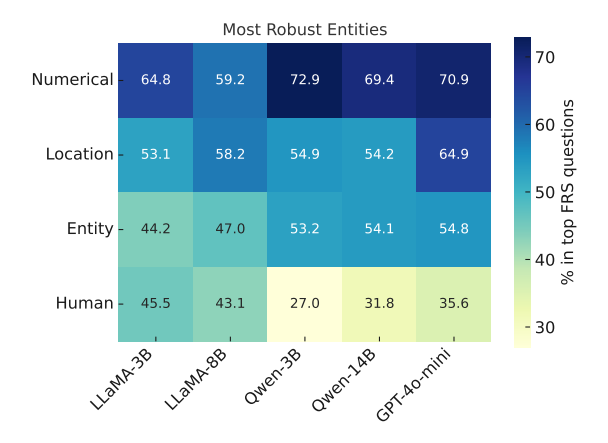


Figure 5: Numerical facts are most robust across all models. Grouping the top most robust answers into question categories across datasets, we show the dominance in % of the categories for each model. Answers to numerical or location-based questions are most robust, while questions about names (here: *Human*) lead to least robust answers.

### 6 Conclusion

This study provides a comprehensive analysis of factual robustness in LLMs and introduces the Factual Robustness Score (FRS) as a novel metric for evaluating factual stability under varying conditions. Unlike traditional accuracy-based assessments, FRS captures both internal generation uncertainty (entropy) and sensitivity to temperature, offering a more nuanced measure of robustness.

Our findings show that increasing temperature reduces factual accuracy, with models that are more confident in their initial answers maintaining correctness longer. However, since entropy alone does not fully predict breaking temperature  $t_b$ , FRS integrates both factors for a more complete evaluation. While larger models generally exhibit greater robustness, architectural and training differences mean that some smaller models outperform their larger counterparts. Additionally, factual robustness varies by knowledge type, with numerical facts proving more stable than others. In a practical sense, FRS holds potential for enhancing a model's factual accuracy through continued pretraining: by evaluating a model's FRS, one can identify areas of weakness (specific facts where the

<sup>&</sup>lt;sup>4</sup>We report details about the dataset and the training procedure in Appendix H.

model underperforms) and use these as targeted data for further training. Beyond introducing FRS, this study highlights limitations in current evaluation methodologies and demonstrates that factual robustness is influenced by both model properties and the nature of the knowledge itself. Future work could explore (1) finding the optimal breaking temperature for each model based on the initial entropy, (2) higher-temperature effects, and (3) strategies for enhancing factual retention to improve the reliability of LLMs in real-world applications.

### Limitations

One key limitation of FRS is the need to evaluate model responses across multiple temperature levels to determine the breaking point  $t_b$ , making the process computationally intensive. Developing more efficient estimation methods to approximate robustness without exhaustive sampling would enhance its practicality. Additionally, we acknowledge that our analysis is constrained by an upper bound of  $t_b = 2.0$ , meaning we cannot determine at which t > 2.0 certain answers would break, leaving some robustness thresholds uncertain - similarly to so far uninvestigated temperatures in-between our chosen values of t. Lastly, our study focuses on question answering in a controlled, closed-book setting, whereas real-world applications often involve external knowledge sources, such as retrievalaugmented generation (RAG) systems, which may further impact factual stability.

### **Ethics Statement**

This work aims to analyze the behavior and reliability of large language models, contributing to a deeper understanding of their factual robustness. While our findings have potential societal implications, we do not identify any immediate ethical concerns that require specific attention. We encourage further discussions on the broader impact of LLM evaluation methodologies.

### References

- David H Ackley, Geoffrey E Hinton, and Terrence J Sejnowski. 1985. A learning algorithm for boltzmann machines. *Cognitive science*, 9(1):147–169.
- Alexander Bondarenko and Adrian Viehweger. 2024. Llm robustness against misinformation in biomedical question answering. *arXiv preprint arXiv:2410.21330*.

- Chung-Ching Chang, David Reitter, Renat Aksitov, and Yun-Hsuan Sung. 2023. Kl-divergence guided temperature sampling. arXiv preprint arXiv:2306.01286.
- Damai Dai, Li Dong, Yaru Hao, Zhifang Sui, Baobao Chang, and Furu Wei. 2021. Knowledge neurons in pretrained transformers. *arXiv preprint arXiv:2104.08696*.
- Nicola De Cao, Wilker Aziz, and Ivan Titov. 2021. Editing factual knowledge in language models. *arXiv* preprint arXiv:2104.08164.
- Saadia Gabriel, Asli Celikyilmaz, Rahul Jha, Yejin Choi, and Jianfeng Gao. 2021. GO FIGURE: A meta evaluation of factuality in summarization. In *Findings of the Association for Computational Linguistics: ACL/IJCNLP 2021, Online Event, August 1-6, 2021*, volume ACL/IJCNLP 2021 of *Findings of ACL*, pages 478–487. Association for Computational Linguistics.
- Mor Geva, Roei Schuster, Jonathan Berant, and Omer Levy. 2020. Transformer feed-forward layers are keyvalue memories. *arXiv* preprint arXiv:2012.14913.
- Dan Hendrycks, Collin Burns, Steven Basart, Andy Zou, Mantas Mazeika, Dawn Song, and Jacob Steinhardt. 2021. Measuring massive multitask language understanding. In 9th International Conference on Learning Representations, ICLR 2021, Virtual Event, Austria, May 3-7, 2021. OpenReview.net.
- Nikolaus HR Howe, Michał Zając, Ian R McKenzie, Oskar John Hollinsworth, Pierre-Luc Bacon, and Adam Gleave. 2024. Exploring scaling trends in llm robustness. In *ICML 2024 Next Generation of AI Safety Workshop*.
- Xuming Hu, Junzhe Chen, Xiaochuan Li, Yufei Guo, Lijie Wen, Philip S Yu, and Zhijiang Guo. 2023. Do large language models know about facts? *arXiv* preprint arXiv:2310.05177.
- Mandar Joshi, Eunsol Choi, Daniel S Weld, and Luke Zettlemoyer. 2017. Triviaqa: A large scale distantly supervised challenge dataset for reading comprehension. In *Proceedings of the 55th Annual Meeting of the Association for Computational Linguistics (Volume 1: Long Papers)*, pages 1601–1611.
- Tom Kwiatkowski, Jennimaria Palomaki, Olivia Redfield, Michael Collins, Ankur Parikh, Chris Alberti, Danielle Epstein, Illia Polosukhin, Jacob Devlin, Kenton Lee, et al. 2019. Natural questions: a benchmark for question answering research. *Transactions of the Association for Computational Linguistics*, 7:453–466
- Xin Li and Dan Roth. 2002. Learning question classifiers. In *COLING 2002: The 19th International Conference on Computational Linguistics*.
- Matéo Mahaut, Laura Aina, Paula Czarnowska, Momchil Hardalov, Thomas Müller, and Lluís Màrquez. 2024. Factual confidence of llms: On reliability

and robustness of current estimators. arXiv preprint arXiv:2406.13415.

Joshua Maynez, Shashi Narayan, Bernd Bohnet, and Ryan T. McDonald. 2020. On faithfulness and factuality in abstractive summarization. In *Proceedings of the 58th Annual Meeting of the Association for Computational Linguistics, ACL 2020, Online, July 5-10, 2020*, pages 1906–1919. Association for Computational Linguistics.

Kevin Meng, David Bau, Alex Andonian, and Yonatan Belinkov. 2022. Locating and editing factual associations in gpt. *Advances in Neural Information Processing Systems*, 35:17359–17372.

Kai Nakaishi, Yoshihiko Nishikawa, and Koji Hukushima. 2024. Critical phase transition in a large language model. *arXiv preprint arXiv:2406.05335*.

OpenAI. 2023. Gpt-4 technical report. arXiv preprint arXiv:2303.08774.

Max Peeperkorn, Tom Kouwenhoven, Dan Brown, and Anna Jordanous. 2024. Is temperature the creativity parameter of large language models? *arXiv preprint arXiv:2405.00492*.

Fabio Petroni, Tim Rocktäschel, Sebastian Riedel, Patrick S. H. Lewis, Anton Bakhtin, Yuxiang Wu, and Alexander H. Miller. 2019. Language models as knowledge bases? In Proceedings of the 2019 Conference on Empirical Methods in Natural Language Processing and the 9th International Joint Conference on Natural Language Processing, EMNLP-IJCNLP 2019, Hong Kong, China, November 3-7, 2019, pages 2463–2473. Association for Computational Linguistics.

Pranav Rajpurkar, Jian Zhang, Konstantin Lopyrev, and Percy Liang. 2016. SQuAD: 100,000+ questions for machine comprehension of text. In *Proceedings of the 2016 Conference on Empirical Methods in Natural Language Processing*, pages 2383–2392, Austin, Texas. Association for Computational Linguistics.

Matthew Renze and Erhan Guven. 2024. The effect of sampling temperature on problem solving in large language models. In *Findings of the Association for Computational Linguistics: EMNLP 2024, Miami, Florida, USA, November 12-16, 2024*, pages 7346–7356. Association for Computational Linguistics.

Adam Roberts, Colin Raffel, and Noam Shazeer. 2020. How much knowledge can you pack into the parameters of a language model? In *Proceedings of the 2020 Conference on Empirical Methods in Natural Language Processing, EMNLP 2020, Online, November 16-20, 2020*, pages 5418–5426. Association for Computational Linguistics.

Victor Sanh, Lysandre Debut, Julien Chaumond, and Thomas Wolf. 2019. Distilbert, a distilled version of bert: smaller, faster, cheaper and lighter. *arXiv* preprint arXiv:1910.01108.

Hugo Touvron, Thibaut Lavril, Gautier Izacard, Xavier Martinet, Marie-Anne Lachaux, Timothée Lacroix, Baptiste Rozière, Naman Goyal, Eric Hambro, Faisal Azhar, et al. 2023. Llama: Open and efficient foundation language models. *arXiv preprint arXiv:2302.13971*.

Xilie Xu, Keyi Kong, Ning Liu, Lizhen Cui, Di Wang, Jingfeng Zhang, and Mohan S. Kankanhalli. 2024. An LLM can fool itself: A prompt-based adversarial attack. In *The Twelfth International Conference on Learning Representations, ICLR 2024, Vienna, Austria, May 7-11, 2024.* OpenReview.net.

An Yang, Baosong Yang, Beichen Zhang, Binyuan Hui, Bo Zheng, Bowen Yu, Chengyuan Li, Dayiheng Liu, Fei Huang, Haoran Wei, et al. 2024. Qwen2. 5 technical report. *arXiv preprint arXiv:2412.15115*.

Zhilin Yang, Peng Qi, Saizheng Zhang, Yoshua Bengio, William W. Cohen, Ruslan Salakhutdinov, and Christopher D. Manning. 2018. Hotpotqa: A dataset for diverse, explainable multi-hop question answering. In *Proceedings of the 2018 Conference on Empirical Methods in Natural Language Processing, Brussels, Belgium, October 31 - November 4, 2018*, pages 2369–2380. Association for Computational Linguistics.

Shimao Zhang, Yu Bao, and Shujian Huang. 2024. Edt: Improving large language models' generation by entropy-based dynamic temperature sampling. *arXiv* preprint arXiv:2403.14541.

Qing Zong, Zhaowei Wang, Tianshi Zheng, Xiyu Ren, and Yangqiu Song. 2024. Comparisonqa: Evaluating factuality robustness of llms through knowledge frequency control and uncertainty. *arXiv* preprint *arXiv*:2412.20251.

# A Temperature Effect on Probability Distribution

Identically to Figure 2, we provide visualizations of the token probability distributions under different temperatures for SQuAD and HotpotQA (see Figures 6 and 7).

### **B** Derivations on FRS

For simplicity of the formulas, we suppose that d = 1, thus we omit it from the equations. However, regardless of the choice of d, the same bounds hold.

### **B.1** Bounds of Equation (3)

Given that  $H \in [0,1]$  and  $t_b \ge 0$ , we first find the minimum and maximum values of Equation (3).

**Case 1:** 
$$t_b = 0$$

$$f(H,0) = (1-H)(0+1) - H \cdot \frac{1}{0+1}$$
$$= (1-H) - H = 1 - 2H$$

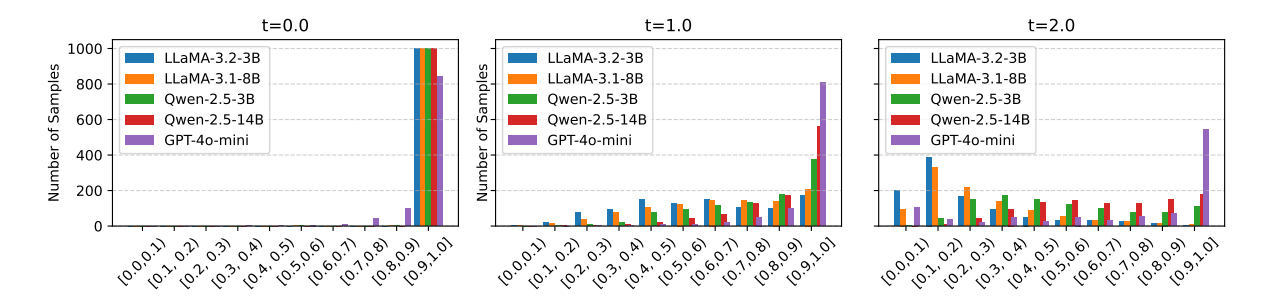


Figure 6: Impact of t on token probability distribution: SQuAD.

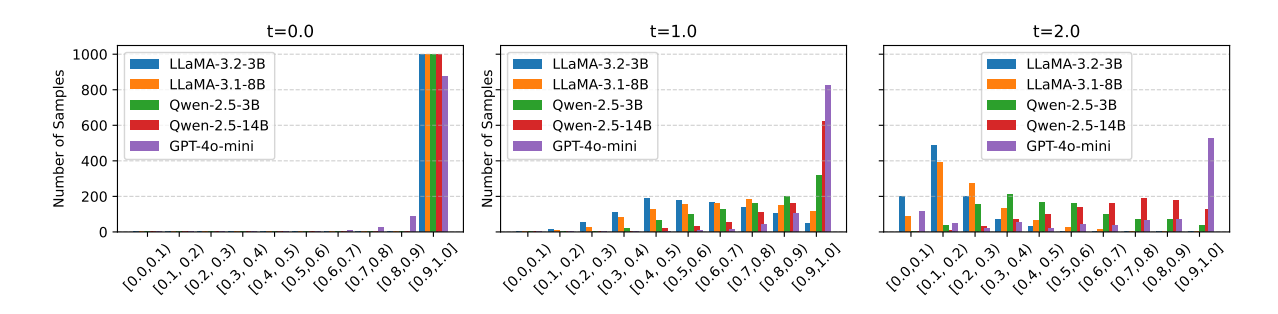


Figure 7: Impact of t on token probability distribution: HotpotQA.

When H=0, we get f(0,0)=1. When H=1, we get f(1,0)=-1. Since f(H,0) is linear in H, the range at  $t_b=0$  is [-1,1].

### Case 2: $t_b \to \infty$

If H<1, we have  $(1-H)\cdot(t_b+1)\to\infty$  and  $\frac{H}{t_b+1}\to 0$ . Thus, when H=0, then  $f(0,t_b)\to\infty$ , and, when H=1, then  $f(1,t_b)\to 0$ .

Summarizing:

- At  $t_b = 0$ , the function is in the range [-1, 1].
- As  $t_b \to \infty$ , the function is in the range  $(0, \infty)$ .
- Since  $f(H, t_b)$  is continuous and monotonic in  $t_b$ , the full range of the function is  $[-1, \infty)$ .

### **B.2** From Equation (3) to Equation (4)

To scale the function

$$f(H, d, t_b) = (1 - H)^d \cdot (t_b + 1) - \frac{H}{t_b + 1}$$

into the range [0,1], we use min-max normalization:

$$f_0^1(H, d, t_b) = \frac{f(H, d, t_b) - f_{\min}}{f_{\max} - f_{\min}},$$
 (5)

where  $f_{\min} = -1$  and  $f_{\max} \to \infty$ . Thus, we define:

$$f_0^1(H, d, t_b) = \frac{(1 - H)^d \cdot (t_b + 1) - \frac{H}{t_b + 1} + 1}{(1 - H)^d \cdot (t_b + 1) - \frac{H}{t_b + 1} + 2}$$
$$= \frac{f(H, d, t_b) + 1}{f(H, d, t_b) + 2}.$$

### C Visual Intuition of FRS

As described in Section 5.1, here we provide a visual intuition of the FRS function. Figure 8 illustrates  $f(H,1,t_b)$  and  $f_0^1(H,1,t_b)$  by ranging the breaking temperature  $t_b \in [0,2]$ . Note how Equation (3) – see left plot – is more aggressive (gives a lower FRS) with  $t_b \rightarrow 2$ , while Equation (4) has a smoother transition to higher FRS. Additionally, we show how d reshapes the FRS function by giving more importance to the initial entropy H – see Figure 9.

# D Effect of d in FRS and its Role in Factual Robustness of LLMs

The exponent d of Equation (3) plays a crucial role in adjusting the sensitivity of the factual robustness measure to entropy H. The term  $(1-H)^d$  introduces a nonlinear scaling effect on the first component  $(t_b+1)$ . The impact of d is analyzed below and illustrated in Figure 9.

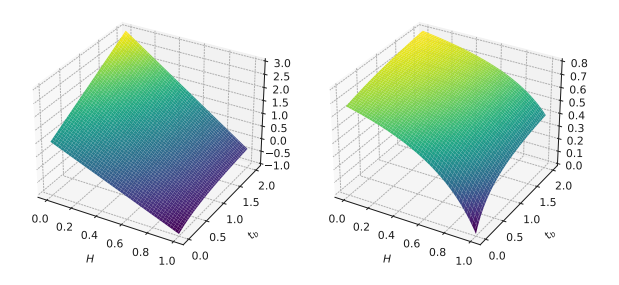


Figure 8: 3D plot of  $f(H, 1, t_b)$  and  $f_0^1(H, 1, t_b)$  over  $H \in [0, 1]$  and  $t_b \in [0, 2]$ . The figure visualizes Equation (3) (left) and Equation (4) (right) where H represents a weighting factor between two competing terms, and  $t_b$  is the breaking temperature. The surface plot highlights how **FRS varies as a function of both parameters**.

# Case 1: d > 1 (Stronger Penalization for High Entropy)

- When d is large, even moderate values of H significantly reduce  $(1-H)^d$ , making the first term in  $f(H,d,t_b)$  much smaller.
- This causes the function to strongly penalize models with high entropy.
- This is desirable because high entropy corresponds to greater uncertainty in the model's responses, making them less trustworthy.

# Case 2: 0 < d < 1 (Smoother Decay of Robustness with Entropy)

- If d is small, the decay of  $(1 H)^d$  is much less aggressive.
- Even models with moderate entropy will not be penalized as strongly.
- This allows models with some uncertainty to still contribute positively to factual robustness.

### Case 3: d = 1 (Linear Dependence on Entropy)

• The function simplifies to:

$$f(H, 1, t_b) = (1 - H)(t_b + 1) - \frac{H}{t_b + 1}.$$
 (7)

• The effect of *H* on robustness is purely linear, with no additional weighting applied to lower-entropy or higher-entropy cases.

# **D.1** Why is d Useful for Evaluating Factual Robustness?

Introducing d allows for greater control over the sensitivity of factual robustness to entropy, making it particularly useful when evaluating the reliability of LLMs under adversarial conditions. When

d>1, models producing uncertain responses  $(H\to 1)$  contribute less to factual robustness, which aligns with the intuition that uncertain responses are inherently less trustworthy. This ensures that models with higher entropy are penalized more aggressively, reflecting their reduced reliability.

Additionally, the robustness score should scale appropriately with  $t_b$ , the breaking temperature at which the model begins to fail. Since the first term in  $f(H,d,t_b)$  is multiplied by  $(t_b+1)$ , models that can withstand higher adversarial pressures before failing naturally receive a higher robustness score. This scaling property ensures that models capable of maintaining factual accuracy under increasing difficulty are recognized as more robust.

Another key advantage of introducing d is that it provides a tunable sensitivity to entropy, allowing for customized evaluation criteria. A high value of d enforces stricter robustness criteria, meaning that even moderate uncertainty is penalized heavily. This is particularly useful in applications where high confidence is required, such as medical AI or legal text generation. Conversely, a lower value of d results in a more lenient evaluation, permitting models with some uncertainty to still be considered reasonably robust. This flexibility makes the function adaptable to various contexts, balancing the trade-off between strictness and tolerance in factual robustness assessment.

In general, d acts as a tuning factor that determines how much we penalize uncertainty when assessing the robustness of an LLM. This flexibility is crucial when evaluating models under different conditions, such as (a) high-stakes applications (e.g., medical AI) where high certainty is required, favoring a high d, and (b) general NLP tasks where moderate uncertainty might be acceptable, allowing for a lower d.

### E Time Complexity Analysis of FRS

To compute the FRS, we consider the following steps:

- 1. Generating an answer using a transformer-based architecture.
- 2. Finding the breaking temperature  $t_b$ .
- 3. Computing entropy H.
- 4. Computing the FRS function itself.

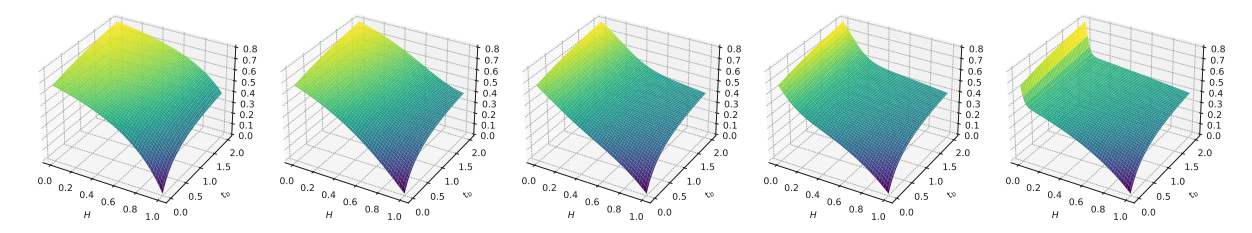


Figure 9: 3D plots of  $f_0^1(H, d, t_b)$  over  $H \in [0, 1]$ ,  $t_b \in [0, 2]$ , and  $d \in \{1, 2, 5, 10, 50\}$  with d varying from the left-most to the right-most subplot.

# E.1 Feeding the Question to the LLM and Generating an Answer

Modern autoregressive LLMs generate text one token at a time. If the model generates an answer of length L, it requires  $\mathcal{O}(L)$  forward passes. Each forward pass involves a Transformer forward computation, which has complexity:

$$\mathcal{O}(L \cdot D^2), \tag{8}$$

where L is the number of generated tokens, and D is the model's hidden size which scales with the number of parameters. Thus, the time complexity for generating one answer is  $\mathcal{O}(L \cdot D^2)$ .

## **E.2** Finding the Breaking Temperature

The breaking temperature  $t_b$  is the point where the model's accuracy falls below a certain threshold – in our case 50%. Determining  $t_b$  requires multiple evaluations.

### **Incremental Search:**

- We test up to  $\mathcal{O}(T)$  different values for  $t_b$ .
- Each requires k model runs.
- Since each model run has  $\mathcal{O}(L \cdot D^2)$  complexity, the total cost is:

$$\mathcal{O}(T \cdot k \cdot L \cdot D^2) \tag{9}$$

### **Binary Search (Optimized Approach):**

- A structured search can reduce the number of evaluations to  $\mathcal{O}(\log T)$ .
- ullet Each evaluation still requires k model runs.
- This reduces the complexity to:

$$\mathcal{O}(k\log T \cdot L \cdot D^2) \tag{10}$$

### **E.3** Computing Entropy

The entropy of a generated sequence is computed as:

$$H = -\sum_{i} P(x_i) \log P(x_i)$$

where  $P(x_i)$  are the token probabilities output by the LLM, and for each of the L tokens, the model

produces a probability distribution over a vocabulary V. Hence, retrieving token probabilities costs  $\mathcal{O}(VL)$  since each token's probability distribution has V elements, and computing the overall entropy has a complexity of  $\mathcal{O}(VL)$ .

### **E.4** Computing the FRS Function

The function

$$f(H, d, t_b) = (1 - H)^d \cdot (t_b + 1) - \frac{H}{t_b + 1}$$

requires basic arithmetic and exponentiation, which are computed in  $\mathcal{O}(1)$ .

### **E.5** Total Time Complexity Per Question

Summing up all contributions:

**Using Binary Search (Optimized):** 

$$\mathcal{O}(k \log T \cdot L \cdot D^2 + VL)$$

### Using Incremental Search (Naïve Approach):

$$\mathcal{O}(T \cdot k \cdot L \cdot D^2 + VL)$$

### **Takeaway**

- LLM inference dominates the complexity, as it requires  $\mathcal{O}(L \cdot D^2)$  per model run.
- Finding  $t_b$  is the most expensive step, since it requires multiple model evaluations.
- Entropy computation  $\mathcal{O}(VL)$  is relatively small compared to LLM inference.
- Binary search significantly reduces complexity from  $\mathcal{O}(T \cdot k)$  to  $\mathcal{O}(k \log T)$ .

# F Extended FRS Results

In Figures 10 to 12, we present the FRS scores for all models across various datasets, considering different values of  $d \in \{1, 2, 5, 10, 50\}$ . As d increases, the influence of entropy H on the FRS

grows, leading to a steady decline in average FRS scores across all models and datasets. This demonstrates the role of the d parameter in systematically downscaling the overall robustness score. However, it is important to note that samples without a detected  $t_b$  remain unaffected, consistently maintaining an FRS of 1.

## **G** Probability Density Functions of FRS

Figure 13 presents the Probability Density Functions (PDF) for all models on SQuAD (top), HotpotQA (middle), and TriviaQA (bottom). Notably, Qwen-14b and GPT-4o-mini exhibit comparable robustness levels. As discussed in the main paper, when a model does not break on a question with  $t_b \leq 2$ , we set FRS=1, which explains the observed gap in the x-axis in the interval [0.8,1). A deeper investigation into higher breaking temperatures beyond 2 could help validate the assigned FRS=1 scores or provide more refined estimates, thereby filling the gap in the plots with more accurate robustness scores.

## **H** Robust Question Types

### **H.1** Training and Dataset

We fine-tune the base uncased version of DistilBERT, available at https://huggingface.co/distilbert/distilbert-base-uncased, on the TREC dataset provided at https://huggingface.co/datasets/CogComp/trec. The training set consists of 5,500 labeled questions, which we use to fine-tune a classifier for categorizing the questions in our own dataset, specifically those associated with the highest and lowest factual robustness scores. Evaluation on the test set (500 questions) yields an accuracy of 96.6% prior to applying the classifier to our data. Table 2 summarizes the hyperparameters used during training.

Table 2: Training hyperparameters for DistilBERT finetuning on the TREC dataset.

Hyperparameter	Value
learning rate	2e-5
batch size	16
epochs	3
weight decay	0.01

The original dataset consists of six entity types: *Numerical, Location, Human, Entity, Abbreviation* and *Description*. In our results, we choose to omit

the latter two types, since they are not sufficiently represented in our data, on average making up only 2.4% and 0.3%, respectively. Hence, in order to avoid poorly supported claims about the robustness of these entity types, we stick with the other four types that are most characteristic of our data.

### H.2 Examples

We provide examples of each question type analyzed in Section 5.3 for further illustration.

### **Numerical**

Q: In what year did Universal make a film version of Dracula?

**A:** 1931

*Numerical*-type questions usually ask for a quantity, a date, or similar. The model's response is usually a single number.

### Location

Q: The Scorpions came from what country?

A: Germany

*Location*-type questions usually ask for a location, like a country, city, or similar. The model's response is a place.

### Human

*Q*: Who introduced the first quantized model of the atom?

A: Niels Bohr

*Human*-type questions usually ask for the name of a person or a group of people. The model's response is a name.

### **Entity**

Q: What is very similar to Valencian and is considered a variety of the same language?

A: Catalan

Q: Guatama discovered the middle path before his what?

A: Enlightenment

Q: What color jersey does Bayern Munich wear?

A: Red

Entity-type questions are not broadly categoriz-

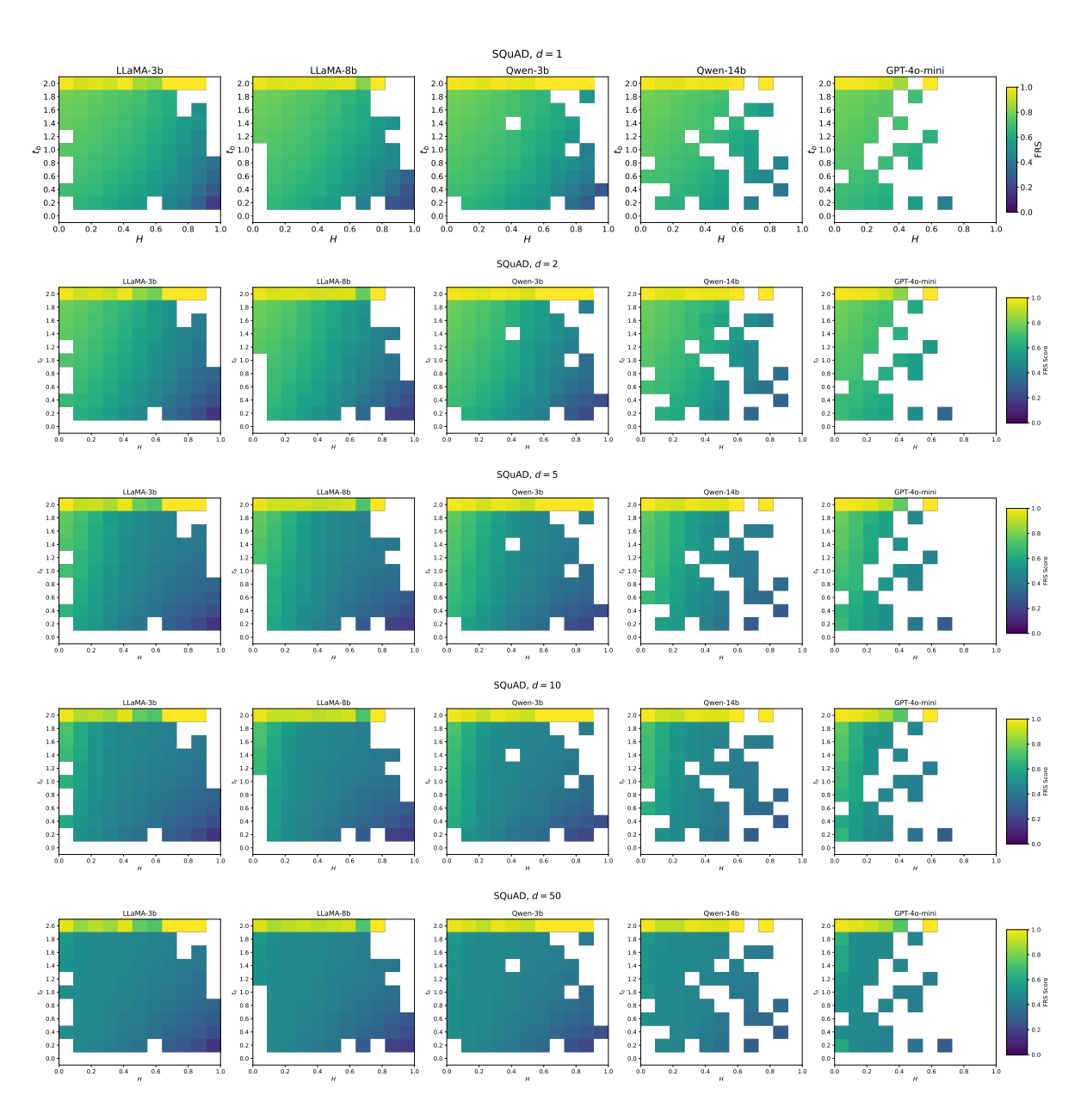


Figure 10: SQuAD. FRS scores across models illustrating effects of  $d \in \{1, 2, 5, 10, 50\}$ .

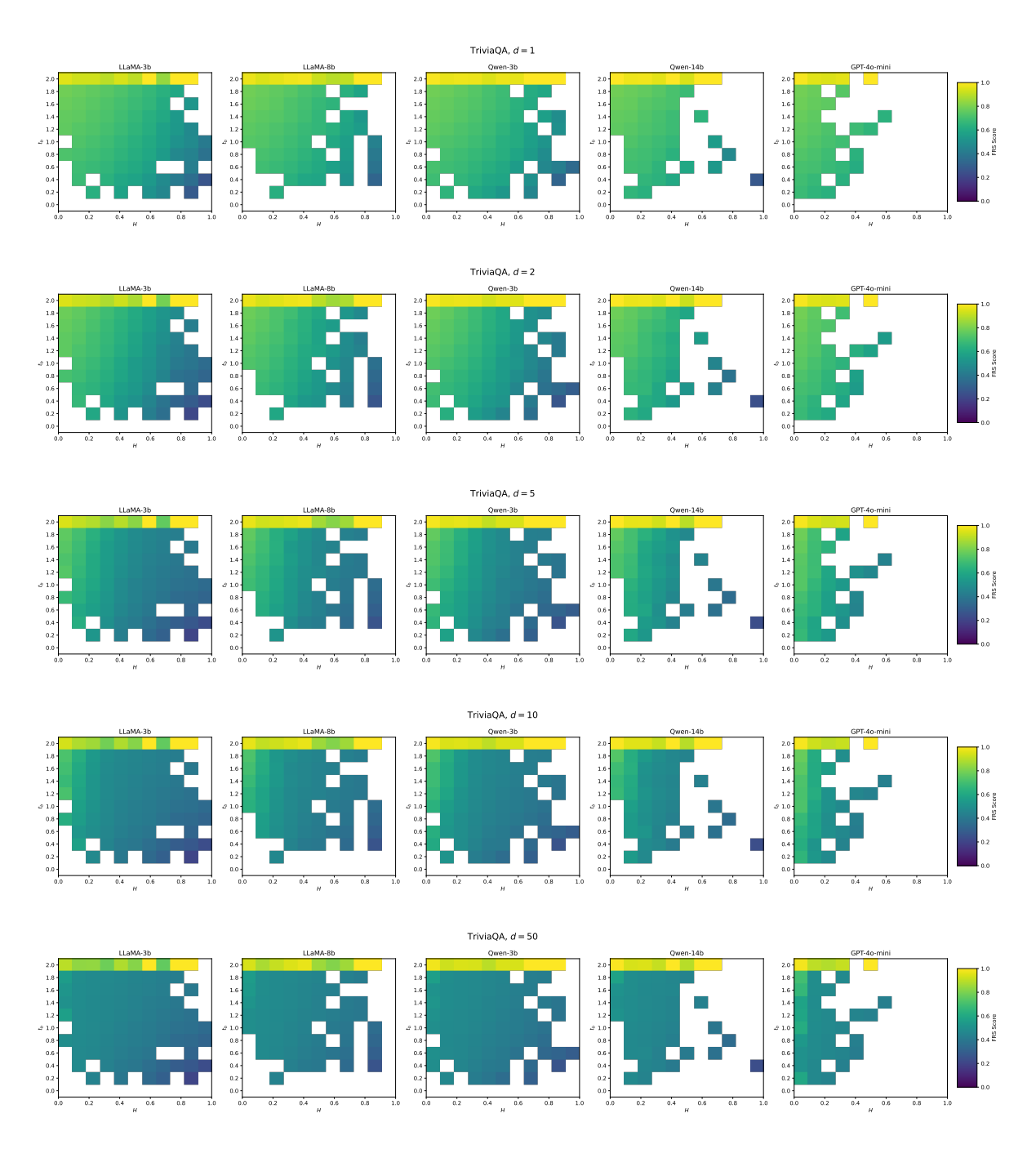


Figure 11: TriviaQA. FRS scores across models illustrating effects of  $d \in \{1, 2, 5, 10, 50\}$ .

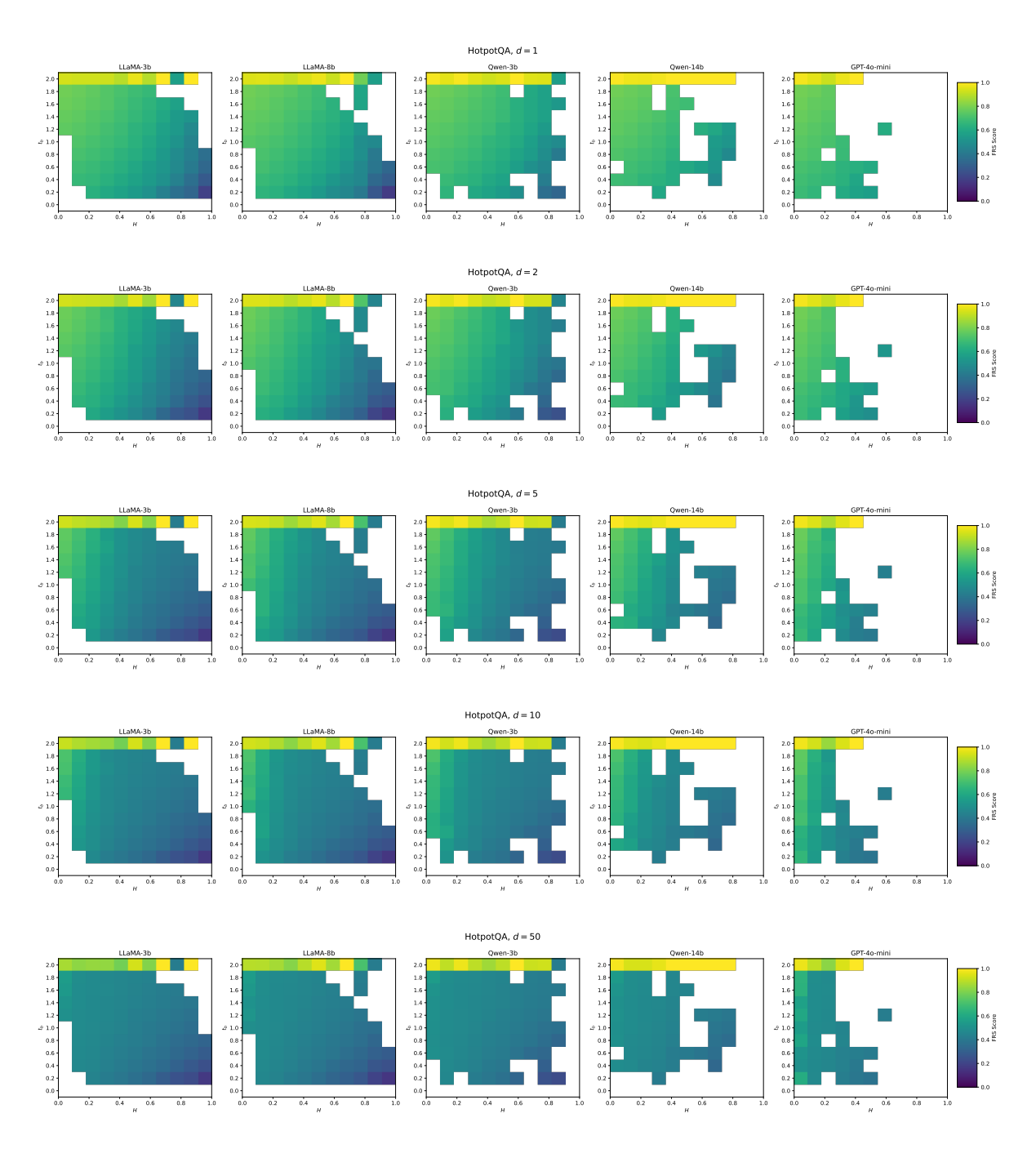


Figure 12: HotpotQA. FRS scores across models illustrating effects of  $d \in \{1, 2, 5, 10, 50\}$ .

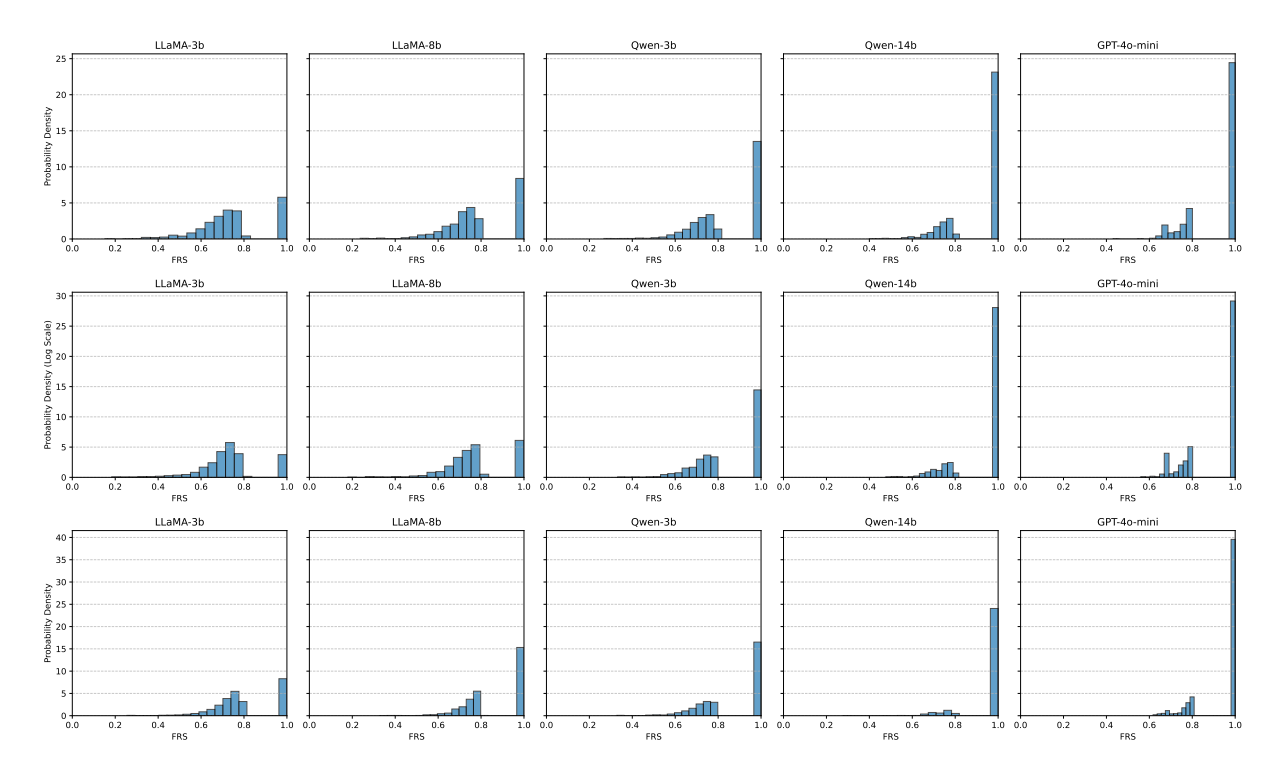


Figure 13: Probability Density Function of FRS for all models on SQuAD (top), HotpotQA (middle), and TriviaQA (bottom).

able. They ask about various facts about the world, which do not typically fall into any of the other categories. For example, they can ask about events, food, language, products. For a full list, see the fine label descriptions on TREC's huggingface dataset card: https://huggingface.co/datasets/CogComp/trec.